University of Nottingham Ningbo China

Mathematics and applied mathematics

Application of Mathematical Methods in Medical Image Analysis: Optimization Strategies for Tumor Detection

Fang Gao, Hongyang Che, Haoyu Wang, Kaiqiao Hu, Xiaowei Chen,

Yibo Lei

November 27, 2024

Contents

Chapter 1

Abstract

This study explores advanced mathematical techniques for optimizing medical image analysis, focusing on enhancing brain tumor detection. By using singular value decomposition, image noise is reduced and key features are preserved to improve diagnostic accuracy. Key tumor features, such as intensity gradient, texture pattern, shape irregularity and contrast. Powerful feature enhancement methods, including contrast normalization and image transformation, further improve image quality. The analysis of the main components was used to reduce dimensionality, retaining 93% of the data variance, while the support vector machine classifier achieved a high accuracy of 93%. Cross validation confirmed that this performance is robust (accuracy 97.4%, AUC: 0.99). Compared to deep learning models, this framework significantly reduces computational requirements for environments with scarce data. The research results have demonstrated the effectiveness of integrating mathematical methods for medical image enhancement and classification, as well as effective tumor diagnosis.

Keywords

Medical Image Analysis, Singular Value Decomposition, Feature, Extraction, Principal Component Analysis, Support Vector Machine

Chapter 2

Introduction

In the field of medical imaging, although advanced technologies such as X-rays, Magnetic Resonance Imaging (MRI), and Computed Tomography (CT) play an indispensable role in providing deep insights into the human body, these technologies face challenges including image noise, unclear features, and an overwhelming volume of images beyond human capacity to review and these challenges have necessitated the use of mathematical methods to enhance the diagnostic process.

In the shift towards disease detection, the field of medical imaging has moved from relying solely on visual inspection to integrating mathematical tools that help improve image quality, enable pattern recognition, and automate anomaly detection, such as tumors and this is crucial for early cancer detection, as recognizing subtle patterns can significantly impact the success of treatment.

This project aims to develop novel mathematical methods for analyzing medical images, focusing on tumor detection. By treating images as matrices, the project leverages linear algebra and optimization techniques to create tools that help clinicians make quicker and more accurate diagnostic decisions and these advancements are essential for managing the growing volume of medical imaging data, enhancing diagnostic accuracy, and improving patient treatment outcomes.

As demonstrated by Litjens et al. (2017)[1], the technologies show excellent performance in classifying and segmenting medical images through advanced machine learning and deep learning models. Furthermore, research by Ronneberger et al. (2015)[2] highlights the efficiency of employing linear algebra and optimization methods in processing and analyzing high-dimensional data and these methods not only improve the accuracy of image interpretation but also play a key role in addressing the challenges brought by the surge in data volumes, supporting clinicians in making earlier and more accurate diagnoses, ultimately providing better treatment options for patients.

Chapter 3

Optimizing Medical Image Enhancement with Singular Value Decomposition

3.1 Method

3.1.1 Singular Value Decomposition

Image enhancement is an essential element in medical image analysis; it helps the health professionals to detect the lesions and make better diagnoses. Traditional visual inspection methods find it difficult to identify key features in noisy images, especially in early cancer detection where fine detail is imperative. Given the development in the computational and the mathematical tools, the matrix decomposition technique that was applied as a part of image processing that seeks to reduce the noise from images and emphasize important components to improve the diagnostic accuracy is Singular Value Decomposition (SVD).[3]

SVD is a method that decomposes a matrix into three components, represented as:

$$A = U\Sigma V^T$$

where A is the original image matrix, U and V are orthogonal matrices, and Σ is a diagonal matrix containing the singular values of the image. The magnitude of these singular values can be interpreted as the weight of the image information; larger singular values generally capture the primary features of the image, while smaller singular values often correspond to noise. We can reduce noise while still maintaining a high image quality by retaining only the major singular values,allowing medical professionals to better identify abnormal regions.

3.1.2 Reconstruction Error (RE)

Reconstruction error (RE) is a measure of the difference between the original and reconstructed images, calculated as:

$$RE = \frac{|A - A_k|_F}{|A|_F}$$

where A_k is the image reconstructed using the top k singular values, and $|A|_F$ denotes the Frobenius norm. A smaller RE indicates a closer approximation of the original image, helping to determine the optimal k for image quality without retaining unnecessary components.

3.1.3 Peak Signal-to-Noise Ratio (PSNR)

PSNR quantifies image quality by comparing the similarity between the original and reconstructed images:

$$PSNR = 20 \cdot \log_{10} \left(\frac{Pixel_{\max}}{\sqrt{MSE}} \right)$$

Where $PSNR_{max}$ is the maximum pixel intensity (255 for an 8-bit grayscale image), and MSE is the mean squared error between the images. A higher $PSNR$ indicates better quality; thus, analyzing $PSNR$ across varying k values and noise levels allows us to assess image enhancement effectiveness.[4]

3.2 Experimental Setup and Results

3.2.1 Dataset and Preprocessed

We used a $256x256$ brain tumor image and Python 3.11 for analysis, loaded and preprocessed in grayscale. The image was subjected to SVD, and different numbers of singular values k were retained for reconstruction.

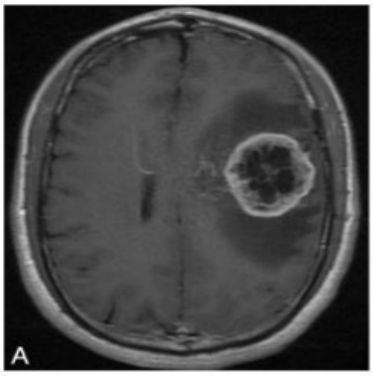

Figure 3.1: A 256x256 brain tumor image

3.2.2 RE and PSNR without Noise

Without interference, the RE consistently decreased as k increased, reaching an elbow point at $k = 50$. Beyond this point, additional singular values contributed less to the image quality, indicating diminishing returns. The $PSNR$ similarly increased with k, eventually stabilizing around $100dB$ as image quality approached the original.

3.2.3 RE and PSNR with Gaussian Noise

RE is almost unaffected by various types of noise interference. With added Gaussian noise (at levels 0.01, 0.05, and 0.1), the $PSNR$ trends remained similar but demonstrated a slower increase at higher noise levels. For instance, at a noise level of 0.1, the $PSNR$ peaked at only 60% of the original image's value beyond $k = 150$, indicating a notable reduction in information retention due to noise. These results highlight how noise impairs enhancement quality, especially at high singular values.

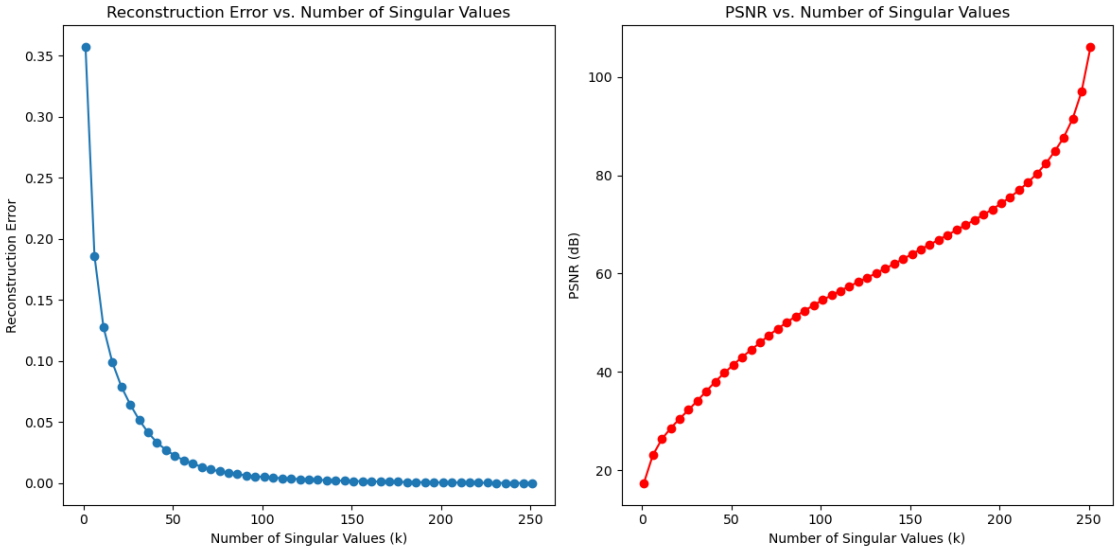

Figure 3.2: RE and PSNR without Noise

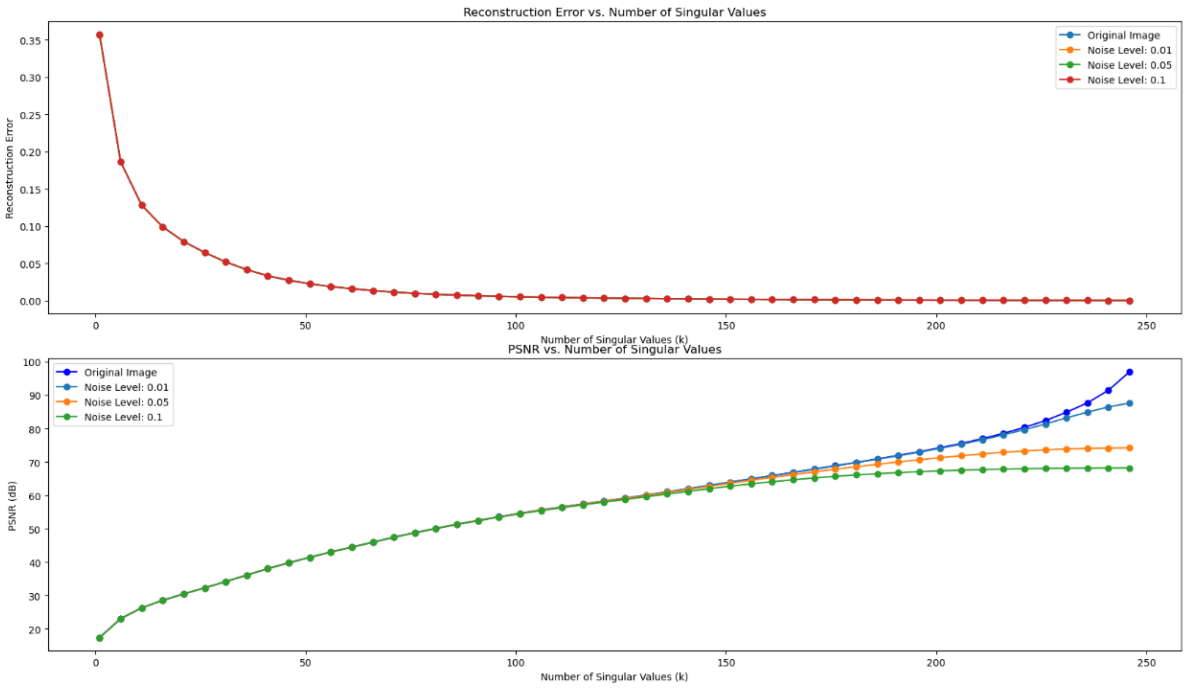

Figure 3.3: RE and PSNR with Gaussian Noise

3.3 Computational Efficiency and Optimization

3.3.1 Computational Trade-offs

Our experiments revealed that computational time increases with the number of singular values k. Full SVD computation on a $256x256$ matrix requires more processing resources.

3.3.2 Optimal k Selection

To balance computational cost and image quality, we found through observation that $k = 75$ was optimal. This value minimizes RE, maintains $PSNR$ within a reasonable range ($50dB$), and reduces the computational burden, ensuring efficient resource usage.

To avoid contingency, two other homologous brain tumor images (256x256) were used for the same procedure. After comparing the result data, it was found that the optimal k value had almost no change, meaning that k = 75 was optimal.

3.4 Conclusion on optimizing image enhancement

This study demonstrated the effectiveness of SVD in enhancing medical images, especially for brain tumor detection. By carefully selecting the optimal number of singular values, SVD enables a balance between computational efficiency and image quality. Future studies could further explore combining SVD with other denoising techniques to enhance robustness in varying noise conditions.

Chapter 4

Optimizing Tumor Detection Through Feature Analysis

4.1 Key Methodologies for Effective Tumor Feature Extraction

The following are the features we used in this section. And before these features are computed, all graphs will be enhanced based on the conclusion of section 3.

4.1.1 Study Intensity Gradients at Tumor Boundaries

Analyzing intensity gradients at tumor boundaries is an important method for tumor detection. By calculating the intensity variations at the edges of tumors, it is possible to effectively identify the presence of tumors. Research shows that the intensity difference between tumors and surrounding normal tissue is often most pronounced at the boundaries, providing crucial clues for tumor localization. The gradient of an image $\nabla I(x, y)$ represents the rate of intensity change at each point (x,y). The gradient is calculated as:

$$\nabla I(x, y) = \left(\frac{\partial I}{\partial x}, \frac{\partial I}{\partial y} \right)$$

Where $I(x, y)$ is the intensity at pixel (x,y), and $\frac{\partial I}{\partial x}and\frac{\partial I}{\partial y}$are the partial derivatives of the intensity function in the x- and y-directions, respectively. The Sobel operator can be used to approximate the gradients:

$$\frac{\partial I}{\partial x} = \sum_{i=-1}^{1} \sum_{j=-1}^{1} S_x(i, j) I(x + i, y + j)$$

$$\frac{\partial I}{\partial y} = \sum_{i=-1}^{1} \sum_{j=-1}^{1} S_y(i, j) I(x + i, y + j)$$

The gradient magnitude $|I(x, y)|$ is used to detect edges, which can represent the rate of intensity change at a given point:

$$|\nabla I(x, y)| = \sqrt{\left(\frac{\partial I}{\partial x} \right)^2 + \left(\frac{\partial I}{\partial y} \right)^2}$$

At tumor boundaries, the gradient magnitude is typically large due to the significant intensity difference between the tumor and the surrounding normal tissue.[6]

4.1.2 Analyze Texture Patterns Using GLCM Matrices

The statistical technique known as the Gray Level Co-occurrence Matrix (GLCM) was introduced by R. Haralick and colleagues in the early 1970s[15]. The GLCM is defined as follows: in an image, it represents the probability that a pixel at position (x, y) has a gray level i, while another pixel at a distance of (dx, dy) in the direction θ has a gray level j. This can be expressed mathematically as:

$$P(i,j \mid d,\theta) = \{(x,y) \mid f(x,y) = i, f(x+dx, y+dy) = j, x, y = 0, 1, 2..., N-1\}$$

where d is the relative distance represented by the number of pixels; θ generally considers four directions, which are 0°, 45°, 90°, and 135°; represents a set,$i, j = 0, 1, 2, , , L-1$, L is the gray level of the image; (x, y) is the pixel coordinate in the image.

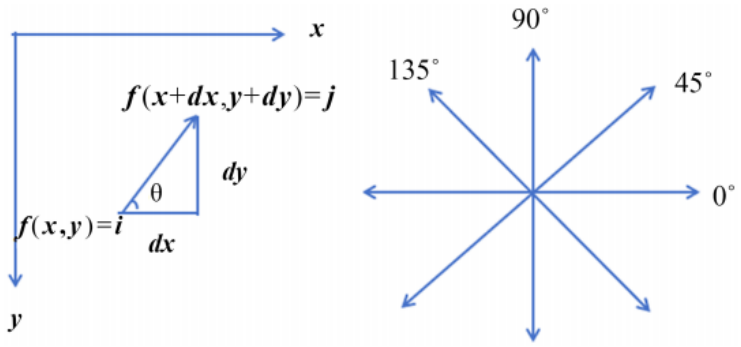

Figure 4.1: Geometric expression of GLCM

As shown in Figure 4.1, the x-direction represents the columns of the image, and the y-direction represents the rows. The term $f(x, y) = i$ denotes the pixel value at coordinates (x, y), and what needs to be counted is the occurrence of the pixel value $f(x + dx, y + dy) = j$ at a distance (dx, dy). Due to different choices of (dx, dy), different angles are considered, typically 0°, 45°, 90°, and 135°, with directions being bidirectional. Given the large dimensions of the gray-level co-occurrence matrix, it is generally not used directly as a feature for texture distinction. Instead, several statistical measures based on it are used as texture classification features. Here, the following 5 statistical measures are utilized:

1) Dissimilarity

Dissimilarity is computed in a way similar to contrast, but instead of increasing exponentially, the weight increases linearly with the distance of the matrix elements from the diagonal. More specifically, the formula for dissimilarity is:

$$\text{Dissimilarity} = \sum_i \sum_j |i-j| P(i,j)$$

where $P(i, j)$ is the probability of the co-occurrence of gray levels i and j.

2) Angular Second Moment (ASM)

The angular second-order moment (ASM) is calculated as the sum of squared elements in the gray level co-occurrence matrix. It represents the uniformity of image grayscale

distribution and texture roughness. When the texture of the image is regular, the values in the gray level co-occurrence matrix tend to cluster in specific regions. For example, in images with continuous gray levels, these values are concentrated near the diagonal, while in structured images, they tend to be far away from the diagonal. In this case, ASM will have a high value. On the other hand, if the values in the co-occurrence matrix are distributed more evenly (such as in noisy images), ASM will be smaller. The formula for ASM is:

$$\text{ASM} = \sum_i \sum_j P(i,j)^2$$

3) Energy

Energy is equal to the Angular Second Moment (ASM):

$$\text{Energy} = \sqrt{\text{ASM}}$$

4) Correlation

Correlation reflects the consistency of image texture. If there is a horizontal texture in the image, the correlation value in the horizontal direction will be greater than in other directions. It measures the similarity between elements of the spatial gray level co-occurrence matrix in the row or column direction. Therefore, the correlation value reflects the local grayscale correlation within the image. When the matrix elements are uniformly equal, the correlation value is large; On the contrary, if the matrix elements have significant differences, the correlation values are relatively small. The formula for Correlation is:

$$\text{Correlation} = \sum_i \sum_j \frac{(i-\mu)(j-\mu)}{\sigma^2} P(i,j)^2$$

where $\mu = \sum_i \sum_j (iP(i,j))/L^2$ is the mean, and $\sigma^2 = \sum_i \sum_j (i-\mu)^2 P(i,j)$ is the variance.

5) Homogeneity

Homogeneity measures the degree of local variation in image texture. If different regions of the image exhibit relatively uniform textures and the textures gradually change, the uniformity value will be high. In contrast, for images with non-uniform textures, the uniformity value will be lower. Unlike comparison, the weights in uniformity decrease exponentially with increasing distance from the diagonal.The formula for homogeneity is:

$$\text{Homogeneity} = \sum_i \sum_j \frac{P(i,j)}{1+(i-j)^2}$$

where $P(i,j)$ is the probability of the co-occurrence of gray levels i and j.

4.1.3 Measure Shape Irregularity Using Circularity Metrics

Shape features are crucial in tumor detection, especially by using circular indices to evaluate the regularity of tumor shape. This index is calculated based on the circumference and area of the tumor, with values close to 1 indicating a more regular shape. Generally speaking, malignant tumors exhibit larger irregular shapes than benign tumors, while benign tumors often have a more uniform shape. This distinction is not only important for preliminary

tumor screening, but also for informing treatment decisions, such as the feasibility of surgical resection. In addition, combining shape features with other biomarkers can improve the accuracy of tumor classification, thereby improving diagnostic results. The circular index can be used to quantitatively describe the shape pattern of tumors. The circularity is typically calculated using the following formula:

$$C = \frac{4\pi A}{P^2}$$

Where A is the area of the tumor, P is the perimeter of the tumor and π is the constant. This formula indicates that the circularity index C approaches 1 as the shape becomes more circular, meaning it is more regular. On the other hand, for irregularly shaped tumors, C will be much smaller than 1.

4.1.4 Compare Contrast Ratios with Surrounding Tissue

The contrast ratio with surrounding tissue is an important feature in tumor detection. Tumors typically exhibit a significant contrast difference with surrounding normal tissue, which can serve as an indicator of tumor presence[8]. By analyzing contrast ratios, the detection rate and accuracy of tumors can be effectively improved. Contrast analysis can be performed by calculating the average gray values of the tumor region and its surrounding area, with higher contrast usually indicating the presence of a tumor. Furthermore, combining contrast features with texture features can enhance detection accuracy. Utilizing machine learning algorithms (such as support vector machines and random forests) to classify contrast features can significantly improve tumor detection performance [2]. To quantify the contrast between the tumor and the surrounding tissue, we can define the contrast ratio as the difference in intensity (gray value) between the tumor region and the surrounding tissue area. The Weber contrast ratio can be calculated using the following formula:

$$C = \frac{|\overline{I_T} - \overline{I_S}|}{\overline{I_S}}$$

Where C is the contrast ratio, $\overline{I_T}$ is the average gray value of the tumor region and $\overline{I_S}$ is the average gray value of the surrounding tissue region.[16]

For simple periodic patterns (e.g., textures), there is no large, uniform luminance area that dominates the user's brightness adaptation. Therefore, there is no obvious choice for the denominator in the above statistics. Michelson Contrast was developed for this case:

$$C = \frac{L_{max} - L_{min}}{L_{max} + L_{min}}$$

where L_{max} represents the maximum luminance in the image or pattern. It is the brightest light intensity value in the scene or image. And the L_{min} represents the minimum luminance in the image or pattern. It is the darkest light intensity value in the scene or image.[16]

4.1.5 Investigate Size Distribution Patterns

The size distribution patterns of tumors are also an important detection feature. By analyzing the sizes and distributions of different tumors, specific characteristics of certain tumor types can be identified[9]. For example, certain types of malignant tumors may have larger diameters and uneven size distributions, while benign tumors are typically smaller and more uniform. The statistical analysis of tumor size can be performed using histograms or

distribution graphs, which can provide important information for tumor classification and prognosis when combined with clinical data. Additionally, utilizing deep learning models to analyze the relationship between tumor size and shape can further improve the accuracy of tumor detection[1].

4.2 Methods to enhance the robustness of features

4.2.1 Test invariance methods

Invariance refers to the property that the extracted features remain unchanged under different condition. We tested the feature stability of Weber Contrast and Michelson across eight images. An original image, four images that were continuously rotated by 90 degrees, two images of horizental and vertical flip, one image added Guass noise $N(0, 10^2)$, and one image magnified 1.2 times. The results are as follows:

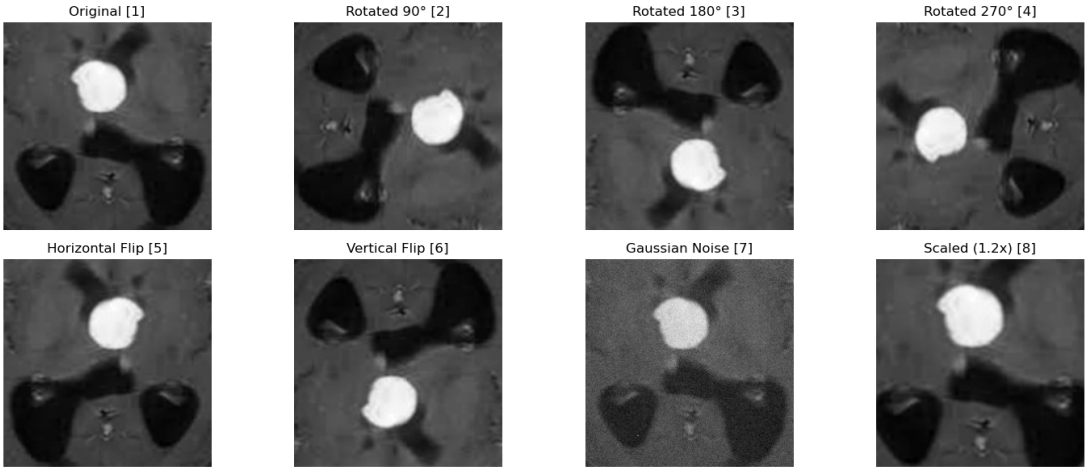

Figure 4.2: Examples of image transformations

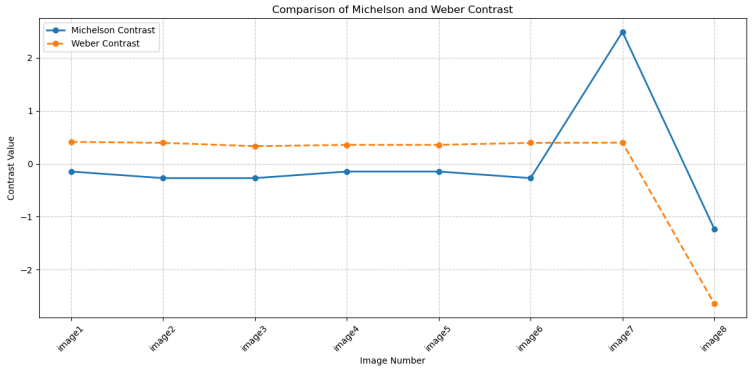

Figure 4.3: Comparison of Micheison and Weber Constract

For rotation and flip, both indicators do not change much, with Weber Contrast is slightly more stable than Michelson Constrast. Michelson Constrasr seems to be more sensitive to the Gauss noise, while Weber is easier to be impact by image scaling. Given our comprehensive analysis, Weber contrast is considered to be more suitable in this case.

4.2.2 Contrast normalization

Contrast normalization is a common image preprocessing method. By adjusting the distribution of pixel values, the dark and light details in the image are more obvious, which improving the visual effect and processing effect.[12] In the field of computer vision and image analysis, contrast normalization can help models process diverse image data more effectively. By contrast normalization, the accuracy of feature extraction can be significantly improved. The normalized images can better adapt to the input requirements of deep learning models and reduce the training time of models.[13]

4.2.3 Otsu automatic threshold segmentation

Otsu automatic threshold segmentation is a usual image segmentation method. It assumes that the image consists of two parts, foreground and background, and that there are two distributions in the grayscale histogram. It separates the foreground and the background from grayscale images. And it calculats the between-class variance for foreground and background, and selects the threshold that maximizes this variance as the optimal threshold. The Otsu algorithm is based on gray histogram, which is relatively computationally small and suitable for real-time processing.[14] Therefore, in the process of determining the contour of the tumor, we firstly used Otsu automatic threshold segmentation method to preprocess the image.

4.3 Result

Figure 4.4 shows the tumor region extracted from a brain tumor MRI scan, including a tumor (the white highlight area) and other tissues. This figure is used to be a sample to demonstrate the computational result below. Before calculating the features, the image is enhanced based on the conclusions of 3.3.2.

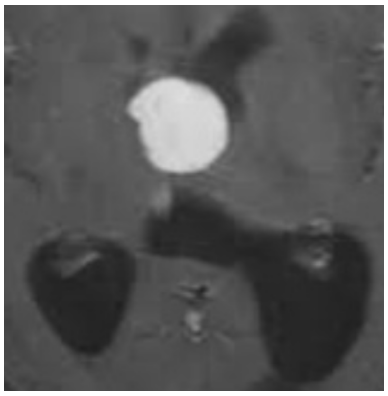

Figure 4.4: Image extracted from a brain tumor MRI scan

4.3.1 The Intensity Gradients

The Sobel operator is used to compute the intensity gradient over the image. The whole calculating process is done by Python, and the result is shown below. From the figure 4.5, we can conclude that the intensity gradient of the tumor boundary is significantly stronger than that of other areas.

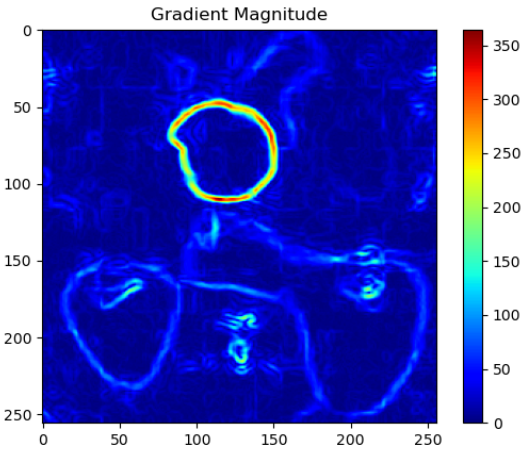

Figure 4.5: The intensity gradient over the image

4.3.2 Value computed by GLCM matrices

The contrast of this image is high, indicating that there are obvious grayscale differences in the image. The high Dissimilarity value indicates there are clear differences in tissue structure or boundaries in the image. The level of Homogeneity is medium, indicating that the image contains both uniform and non-uniform areas. The low Energy and ASM values show that the image texture is irregular, and the grayscale is scattered. The texture of the image has a strong directionality since the value of correlation is high, which means the tissues structure has a certain regularity. Moreover, there is a high texture complexity, as the value of entropy is high.

Table 4.1: GLCM Statistics Values

Contrast	Dissimilarity	Homogeneity	Energy	Correlation	ASM	Entropy
19.631	2.218	0.490	0.068	0.995	0.005	10.870

4.3.3 Circularity

The circularity of the tumor in this image is around 0.85, which is relatively high. This indicated that the tumor's growth is relatively uniform and regular.

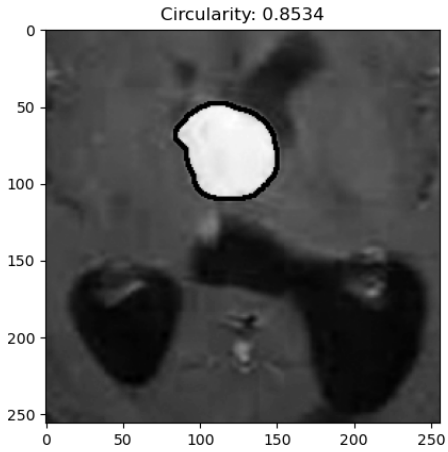

Figure 4.6: Tumor with contour and circularity

4.3.4 Contrast ratios with surrounding tissue

Firstly, the distribution of the grayscale in the tumor and surrounding area were investegated. Figure 4.7 below shows the histogram and the boxplot of grayscale value within these two area. The grayscale of the tumor is significantly higher, with average among 240, and shows a right-skewed distribution. While the gray value in the surrounding area is lower, with mean around 80, and shows a unimodal normal distribution. There is almost no overlap between them, indicating that the grayscale can be an effective feature to distinguish tumor from normal tissue.

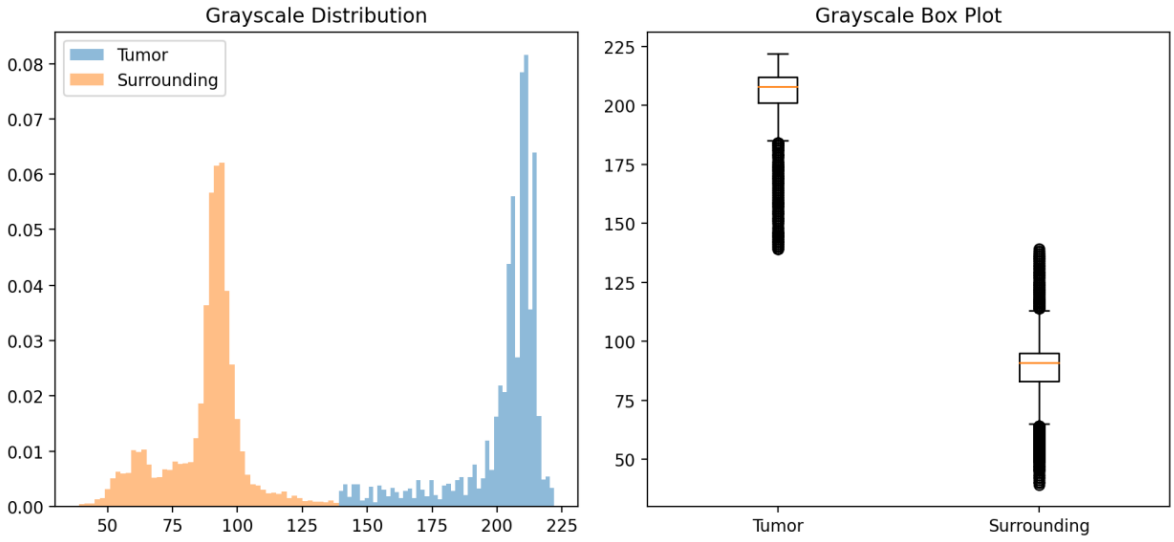

Figure 4.7: Statistical distribution of grayscale values

Therefore, to make use of the gray value, Weber Contrast was introduced. Steps were taken in the following to calculate contrast by programming.

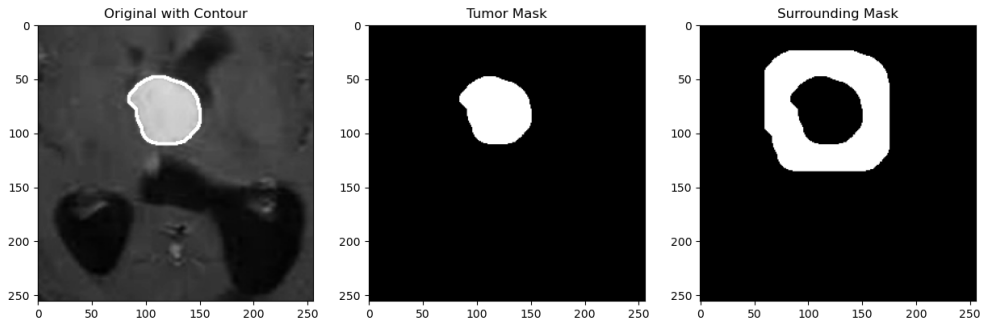

Figure 4.8: Process of calculating contrast

Two masks were generated to extract gray value within the tumor and the surrounding area. First, the tumor area is determined by the contour and a tumor mask is generated. Then, in order to analyze the tissue characteristics around the tumor, a 50×50 square kernel is used to perform morphological dilation on the tumor boundary, expanding it outward by 50 pixels to generate a surrounding mask. After that, the gray value of the tumor area and its surrounding tissue area can be extracted by multiplying these two masks seperately with the original image. Finally, the conctrast ratio was calculated to be approximately 1.32.

4.4 Reduce the dimensionality and classify the features of the model for prediction

In this model, SVM is used for classification based on reduced dimensional features. The PCA processed data simplifies the input of the model, while SVM can fully utilize these features for classification, which helps to improve accuracy and stability in tumor image detection.

4.4.1 Principal Component Analysis

PCA (Principal Component Analysis) is a linear dimensionality reduction method primarily used to reduce the dimensionality of data while preserving as much information as possible from the original data. Mathematically, PCA projects data onto a new coordinate system by solving the eigenvalues and eigenvectors of the covariance matrix, such that the variance in the direction of the first principal component is the largest, the variance in the direction of the second principal component is the second largest and so forth.[10]

4.4.2 Support Vector Machine

SVM (Support Vector Machine) is a supervised learning algorithm based on the principle of minimizing structural risk, which improves the generalization ability of the model by maximizing the decision boundary of sample classification. Mathematically, SVM achieves classification by constructing a hyperplane that maximizes the separation of samples from different categories. For nonlinear separable data, SVM uses kernel functions to map the data to a high-dimensional space, allowing it to be linearly separated in that space.[11]

4.5 Experimental procedure

4.5.1 Data preparation and segmentation

We first preprocess the image dataset, grayscale it, and extract the feature matrix. Next, divide the dataset into a training set and a testing set, using 75% as the training set and 25% as the testing set. In addition, the use of data augmentation (including rotation, flipping, scaling and added Gaussian noise) increases sample diversity, thereby enhancing the robustness of the model.

4.5.2 Feature extraction and standardization

Use multiple image feature extraction methods, including GLCM (gray level co-occurrence matrix) features, gradient features, etc., to ensure feature diversity and effectiveness. Subsequently, the extracted features are standardized to ensure that different features are at the same scale.

4.5.3 Dimensionality Reduction Processing

After data standardization, PCA is applied to retain 90% of the variance, thereby reducing feature dimensions and improving the computational efficiency of the model. PCA not only reduces feature redundancy, but also helps to reduce noise in the data, making the training results more stable.

4.5.4 SVM classification and cross validation

Train the classification model using SVM and apply 5-fold cross validation to evaluate the robustness of the model. In the test set, evaluate the accuracy of the SVM classifier and measure the performance of the model, SVM uses Sigmoid kernel function.

4.6 Experimental results

In order to validate the effectiveness of the proposed feature fusion method for small-sample image classification, we use accuracy, precision, recall, and F1 score to evaluate the results. Their formulas are as follows:

$$\text{accuracy} = \frac{TP + TN}{TP + FP + TN + FN}$$

$$\text{precision} = \frac{TP}{TP + FP}$$

$$\text{recall} = \frac{TP}{TP + FN}$$

$$f_1 = 2\,\frac{\text{precision} \times \text{recall}}{\text{precision} + \text{recall}}$$

Where TP(True Positive) represents the number of correctly predicted positive samples; FP(False Positive) represents the number of negative samples incorrectly predicted as positive; TN(True Negative) represents the number of correctly predicted negative samples; FN(False Negative) represents the number of positive samples incorrectly predicted as negative. In this case, brain tumor images are considered as positive samples, and normal images are considered as negative samples.

PCA reduced the dimensionality of the data to four main features, and explained variance ratio: 0.58871019, 0.151552, 0.10372117, 0.04863917. The experiment showed that the accuracy of the model on the test set reached almost 93%. The accuracy, recall, and F1 score of the SVM classifier is shown in the following table, demonstrating its superior performance in classification tasks. Through cross validation, the average accuracy of SVM was 97.4%, further verifying the stability and robustness of the model.

Class	Precision	Recall	F1-score	Support
Tumor	1.00	0.85	0.92	13
No Tumor	0.89	1.00	0.94	17
Accuracy			0.93	30
Macro avg	0.95	0.92	0.93	30
Weighted avg	0.94	0.93	0.93	30

Table 4.2: Classification Report

4.7 Evaluation

4.7.1 Confusion matrix

The confusion matrix is used to describe the classification performance of a model, including the number of correct and incorrect classifications in the classification task.

4.7.2 Receiver Operating Characteristic Curve (ROC)

The ROC curve is used to evaluate the performance of classification models at different thresholds, showing the relationship between True Positive Rate (TPR) and False Positive Rate (FPR). The shape of the curve: The orange ROC curve displays the overall performance of the model. The closer the ROC curve is to the upper left corner, the better the model performance.

4.7.3 Evaluate conclusion

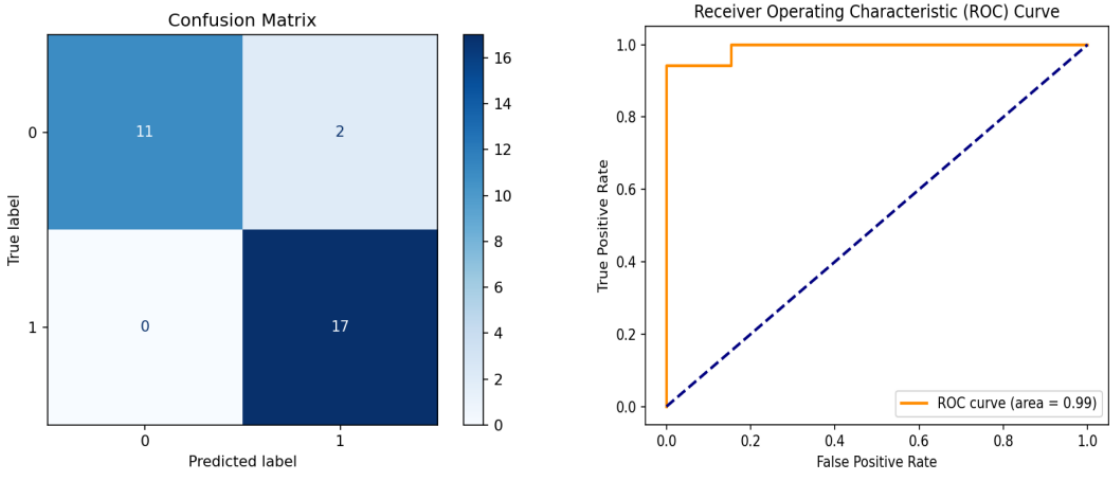

The model performs well and correctly classifies most of the samples. Only 2 samples without tumors were mistakenly identified as having tumors, indicating that the model has some errors in distinguishing negative classes. The AUC value of 0.99 indicates that the model has a very high ability to distinguish positive and negative samples, and its performance has almost reached perfection.

The results of this experiment demonstrate the effectiveness of the model combining PCA and SVM in medical image classification. PCA dimensionality reduction not only reduces feature redundancy, but also improves data separability, while SVM classifier performs well in tumor recognition tasks.

Chapter 5

Discussion and Conclusion

This study has certain limitations. The applicability of this model is also limited by the limited sample size and narrow focus on specific tumor types, as it requires image preprocessing and cannot accurately identify the entire brain tumor image. From a methodological perspective, this model relies on relatively simple techniques and is not sufficient to handle complex scenarios; Future work may adopt more advanced methods, such as Convolutional Neural Networks (CNN). Despite these limitations, the project has enormous potential for expansion. It can further develop into the classification of benign and malignant tumors, and utilize its ability to identify tumor boundaries as a tool to advance research on predicting tumor growth patterns.

This study highlights significant advances in using mathematical methods for brain tumor diagnosis while addressing challenges in medical imaging. This method integrates singular value decomposition (SVD) for image enhancement, gray level co-occurrence matrix (GLCM) for image analysis, principal component analysis (PCA) for feature reduction, and support vector machine (SVM) for classification, with an accuracy of 93%, cross validation accuracy of 97.4%, and AUC of 0.99. This method avoids the high data and computational requirements of deep learning models and surpasses traditional methods in feature extraction efficiency. Future research can explore other classification techniques such as random forest, logistic regression, KNN, and CNN to further improve diagnostic accuracy. The proposed method and optimization strategy have significant clinical value, providing a foundation for faster and more accurate diagnostic decisions in medical image analysis.

Reference

[1] Litjens, G., et al. (2017). A survey on deep learning in medical image analysis. *Medical Image Analysis*, *42*, 60–88.

[2] Ronneberger, O., Fischer, P., & Brox, T. (2015). U-Net: Convolutional networks for biomedical image segmentation. In *International Conference on Medical Image Computing and Computer-Assisted Intervention (MICCAI)* (pp. 234–241). Springer.

[3] Prasantha, H. S., Shashidhara, H. L., & Murthy, K. B. (2007). Image compression using SVD. In *International Conference on Computational Intelligence and Multimedia Applications (ICCIMA 2007)* (Vol. 3, pp. 143–145). IEEE.

[4] Hore, A., & Ziou, D. (2010, August). Image quality metrics: PSNR vs. SSIM. In *2010 20th International Conference on Pattern Recognition* (pp. 2366–2369). IEEE.

[5] Roosta, S. H. (2012). *Parallel processing and parallel algorithms: Theory and computation*. Springer Science & Business Media.

[6] Somkantha, K., et al. (2011). Boundary detection in medical images using edge following algorithm based on intensity gradient and texture gradient features. *IEEE Transactions on Biomedical Engineering*, *58*(3), 567–573.

[7] Haralick, R. M., Shanmugam, K., & Dinstein, I. (1973). Textural features for image classification. *IEEE Transactions on Systems, Man, and Cybernetics*, *3*(6), 610–621.

[8] Monika, A., et al. (2014). Optimized contrast enhancement for tumor detection. *International Journal of Imaging Systems and Technology*, *24*(3), 687–703.

[9] Keiichi, H., et al. (2017). Mo1191 endoscopic features of early duodenal adenocarcinoma/adenoma: Tumor size, microvascular/microsurface pattern, and distribution of white opaque substance. *Gastrointestinal Endoscopy*, *85*(5), AB456–AB457.

[10] Kurita, T. (2019). Principal component analysis (PCA). In *Computer Vision: A Reference Guide* (pp. 1–4). Springer.

[11] Wang, H., & Hu, D. (2005, October). Comparison of SVM and LS-SVM for regression. In *2005 International Conference on Neural Networks and Brain* (Vol. 1, pp. 279–283). IEEE.

[12] Pizer, S. M., Amburn, E. P., Austin, J. D., Cromartie, R., Geselowitz, A., Greer, T., . . . & Zuiderveld, K. (1987). Adaptive histogram equalization and its variations. *Computer Vision, Graphics, and Image Processing*, 39(3), 355-368.

[13] Fleming, A. D., Philip, S., Goatman, K. A., Olson, J. A., & Sharp, P. F. (2006). Automated microaneurysm detection using local contrast normalization and local vessel detection. *IEEE Transactions on Medical Imaging*, 25(9), 1223-1232.

[14] Xu, X., Xu, S., Jin, L., & Song, E. (2011). Characteristic analysis of Otsu threshold and its applications. *Pattern Recognition Letters*, 32(7), 956-961.

[15] Haralick, R. M., Shanmugam, K., & Dinstein, I. H. (1973). Textural features for image classification. *IEEE Transactions on Systems, Man, and Cybernetics, SMC-3*, 610-621. https://doi.org/10.1109/TSMC.1973.4309314

[16] Mogford, R. (n.d.). Luminance contrast. *NASA Ames Research Center, Human Systems Integration Division*.

Image citation:
https://www.kaggle.com/api/v1/datasets/download/ammarnassanalhajali/brain-tumor